A revised photocatalytic transformation mechanism for chlorinated VOCs: experimental evidence from C2Cl4 in the gas phase

A revised photocatalytic transformation mechanism for chlorinated VOCs: experimental evidence from C_2Cl_4 in the gas phase

M. Minella, M. Baudino, C. Minero*

Department of Chemistry and NIS Center of Excellence, University of Torino, Via P. Giuria 5, Torino 10125, Italy, http://www.environmentalchemistry.unito.it.

* Corresponding author. Fax +39-011-6705242; E-mail: claudio.minero@unito.it.

Abstract

The photodegradation of gaseous perchloroethylene (PCE) was investigated on titanium dioxide under UV light at 365 nm at the gas/solid interface in a CSTR photo-reactor (Continuous Stirred Tank Reactor). The rate and products are strongly affected by oxygen presence. Gaseous products of PCE degradation agree with literature. The production of active chlorine (sum of Cl_2, HClO, ClO and ClO_2) was investigated both in the presence of oxygen and in anoxic conditions. At low O_2 concentration no gaseous active chlorine was determined, while a significant amount was measured in the presence of oxygen. By considering that in the absence of O_2 the only possible form of active chlorine is Cl_2, this highlights that $Cl^{\bullet}$ is not produced, and that chain reactions promoted by the chlorine radical do not occur on the TiO_2 surface.

The photocatalytic transformation of C_2Cl_4 was investigated at different concentrations. The rate follows a first order kinetic that is rationalized with a photocatalytic kinetic model in which the substrate is able to react simultaneously with both photogenerated holes and electrons. In anoxic conditions adsorbed halogenated organic compounds with molecular weights higher than that of PCE were produced and chloride ions accumulated at the surface. Reductive pathways have a key role in PCE degradation. The water vapor has a detrimental role on the PCE transformation rate due to the competition with PCE adsorption on reactive sites with 2:1 stoichiometry.

The addition of chloride ions on TiO_2 surface slows down the PCE degradation rate and the production of gaseous CCl_4 but increments that of C_2Cl_6 in anoxic conditions. This is rationalized by a mechanism in which direct hole transfer to substrate occurs followed by chloride anion addition to the carbocation.

Keywords

Photocatalysis, Titanium Dioxide, Perchloroethylene, Chlorine radical, Gas/solid interface, Active chlorine

1 Introduction

The photocatalytic process is a well-known method for abatement of air pollutants. Early studies showed that alkanes, aromatic hydrocarbons, alcohols, aldehydes, ketones, and halogenated solvents can be degraded although in a different extent. The studies on halogenated solvents, namely trichloroethylene (TCE), tetrachloroethylene (PCE) and chloroform date at late 80's.[1] The main products observed were DCAC (dichloroacetyl chloride), $COCl_2$ (phosgene), CO_2, CO and HCl. Nimlos et al. [2] were also able to identify Cl_2 using a molecular beam mass spectrometer. In the degradation of TCE and PCE, $CHCl_3$ and CCl_4 [3,4] were formed as the O_2 mole fraction in the feed gas decreases. The formation of more halogenated products was ascribed to the initial formation of $Cl^{\bullet}$ radicals, and the subsequent preferential attack at the -CHCl side.[3] Comparison of literature data [5] under similar conditions and reactor configuration using the Langmuir Hinshelwood model showed that toluene, m-xylene, acetone and TCE have similar order of magnitude rate constant and apparent binding constant.[6] A photocatalytic rate enhancement for the conversion of many pollutants was reported when co-fed with chloro-olefins.[7] Quantum yield greater than 1 has been cited several times [1,8], although the original papers are almost not available. A detailed mechanism was also proposed through ab initio molecular orbital calculations, showing that addition of $^{\bullet}OH$ and $Cl^{\bullet}$ radicals to TCE is possible, being the first more exothermic than the second one.[3,8] Nowadays, PCE and TCE are still used as model pollutants for reactor configuration studies.[9]

The positive synergic effect, the formation of more halogenated intermediates, and the cited quantum yield greater than 1 for chlorinated compounds were ascribed to chain reactions promoted by the chlorine radical that is formed at the TiO_2 surface.[3,10] The chlorine radical can be formed a) from chloride oxidation by $^{\bullet}OH$ or holes, or b) directly released from oxidized intermediates. The supposed $Cl^{\bullet}$ formation by hydroxyl radicals produced at the surface of TiO_2 exposed to near-UV irradiation in the presence of adsorbed water vapor [11] was able to justify the observed intermediates.[8] The role of chlorine radical was also supported by experiments in which chloride ions were added in the gas phase or at the surface. After addition of HCl in catalytic quantity in the air flow or by PCE overheating, a sensible increase of the reaction rate was obtained.[12] The addition of surface Cl^{-} through prechlorination with HCl increased the rate for toluene and hexane at the very beginning of the reaction when compared to the co-feeding with TCE, for which the enhancement was observed after some reaction time needed to accumulate a useful surface Cl^{-} level.[13]

The chain reaction mechanism assumes that chorine radical is an initiator which adds to TCE, forming a more halogenated radical, which in some further steps releases $Cl^{\bullet}$ or HCl after reaction with oxygen.[3] The chain is terminated when $Cl^{\bullet}$ reacts with water to form $^{\bullet}OH$ (a reaction possible only for pH > 2-2.5 as suggested by the standard redox potential for the couples $E^{o}(Cl^{\bullet}/Cl^{-})$= 2.60 V and $E^{\circ}(^{\bullet}OH,H^{+}/H_2O)$=2.73 V [14]), or in dry conditions to form Cl_2.[15] Chlorine radical could also be depleted by photoelectrons in the conduction bands (reducing to chloride ion that is adsorbed on the surface) or by reaction with O_2, forming ClO_2.[3]

The aforementioned framework based on the key role of $Cl^{\bullet}$ seems to be consistent. However, parallel to earlier studies, alternative explanations could be suggested. For example, literature-reported values of photon efficiency are consistent with a photocatalytic mechanism

without chain reactions mediated by $Cl^{\bullet}$ radical. Using a fluorescence UV source and potassium ferrioxalate actinometry, the TCE photon efficiency was calculated as 13% over conditioned catalysts.[16] Jacoby et al.[1,2] measured quantum yields from 0.5 to 0.8 under high TCE concentration. In addition, the inhibition of the rate in the presence of halide ions in aqueous solution was suggested to be due to the competition with organic molecules for the oxidative species (i.e. photogenerated holes).[17] The chlorine radical, if formed, is subjected to rapid recombination with conduction band electrons, creating a short-circuit cycle that depresses the conversion. An analogous inhibition was observed in the gas-phase photocatalytic degradation of $CHCl_3$ due to the increase of surface Cl^- with the space time.[18] The photoactivity was recovered washing the catalyst. Recently, EPR measurements were conducted to detect the presence of chlorine radicals by using the PBN spin-trap in chloroform solution.[19] The PBN–$Cl^{\bullet}$ radical was not identified, suggesting that the existence of chlorine radical can be largely disregarded, although not completely excluded. Then the rate decrease was ascribed to the surface sites occupancy without a redox involvement of chloride ion. If so, also the formation of $^{\bullet}OH$ radicals, more endoergonic, could hardly be suggested.

The existence of $^{\bullet}OH$ radicals in photocatalysis was debated for years.[20] Although free $^{\bullet}OH$ is still often invoked in the recent literature, the surface trapped hole is most probably the reactive species, often indistinguishable as reactivity from $^{\bullet}OH$ radical. In the photocatalyzed oxidation of TCE in the presence of $^{18}O_2$, oxygen-18 is incorporated into DCAC, phosgene, and CO, indicating that only the oxygen from the gas phase is involved in the oxidation of TCE, whilst oxygen-16 from $H_2{}^{16}O$ is not incorporated in the photooxidation products.[21] This proved that $^{\bullet}OH$ driven oxidation mechanism is not operative in the photooxidation of TCE. The direct electron transfer from organic substrate to the photogenerated holes was recently demonstrated as a unique electron transfer mechanism in the case of photocatalytic transformation of melamine, which is unreactive toward $^{\bullet}OH$ radical.[22] This indicates that direct electron transfer from the surface trapped hole could be in general the sole process responsible for oxidation.[23] Consistently, the product analysis obtained with O_2-sensitised photo-oxidation of indane and some of its hetero-analogs in deaerated CH_3CN and in the presence of Ag_2SO_4 was explained with the intervention of a carbocation in the first reaction event resulting from an electron-transfer mechanism (from the substrate to the photogenerated hole).[24]

To clarify the possible role of $^{\bullet}Cl$ radical some new data on intermediate formation in the photocatalytic degradation of PCE are here reported, both in the presence and absence of O_2, together with the analysis of kinetic data. The formation of gaseous Cl_2 is assessed by a simple trapping experiment.

2 Materials and Methods

Details on used materials, preparation of the catalyst, and experimental setup are reported in Supplementary Material (hereafter SM). The experiments of PCE transformation were carried out in a homemade flow-through photo-reactor working in a regime of perfect mixing (Continuous Stirred Tank Reactor, CSTR, see SM under 1.4).[25,26] Under steady state the output concentration of gaseous C_2Cl_4 does not change with the time, if there is no change in the photoactivity of the catalyst, e.g. no poisoning or photo-activation as a consequence of the irradiation. Consequently, defining the conversion at the time t as $\eta(t)= (C_o-C_{out}(t))/C_o$, where

C_o is the feed concentration and C_{out} the concentration inside the reactor and measured at its outlet, the rate under stationary conditions is directly obtained from the experiment (eq. 1).[25]

$$Rate(C_{out}) = \frac{C_0 \eta_\infty F}{S} \qquad \text{(eq. 1)}$$

The monitoring of C_2Cl_4 flowing out of the reactor was carried out with a Photo Ionization Detector. The volatile VOCs were analysed through both GC-MS after cryofocusing and directly through an FTIR spectrophotometer equipped with a cell for gases with 8 m long optical path length. The catalyst surface modification was assessed through UV-Vis reflectance spectra and FT-IR. The surface-deposited compounds have been extracted and analysed with GC/MS and IC. All details are reported in SM.

The determination of the active chlorine formed during the photocatalytic test was carried out according to a standard spectrophotometric methods,[27] based on the reaction of active chlorine (Cl_2/HClO/ClO^-/ClO) with N,N-diethyl-p-phenylenediamine (DPD). This reaction produces a pink coloured species that can be quantified spectrophotometrically at 510-515 nm. The gas flowing out of the reactor was bubbled through a fritted glass in a slightly basic solution (NaOH 2 mM). This solution favoured the trapping of volatile active chlorine species through: 1) deprotonation of the volatile hypochlorous acid into the non-volatile hypochlorite anion; 2) dismutation of Cl_2 into Cl^- and reactive ClO^- ($Cl_2 + 2\ OH^- \rightarrow H_2O + Cl^- + ClO^-$); 3) reaction of ClO with the excess of hydroxyl ions to form ClO^- ($ClO^\bullet + OH^- \rightarrow ClO^- + {}^\bullet OH$); 4) dismutation of ClO_2 in chlorite and chlorate species ($2\ ClO_2 + H_2O \leftrightarrows HClO_2 + HClO_3$, $K=1.2\times10^{-7}$). At different irradiation times a fixed volume of the solution was withdrawn and mixed with DPD solution buffered at pH 6.2 (phosphate buffer, 0.17 $mol\cdot L^{-1}$ HPO_4^{2-} e 0.33 $mol\cdot L^{-1}$ H_2PO_4). The DPD produced pink colored species was quantified at 510 nm with a Cary 100 UV-Vis spectrophotometer.

3 Results and Discussion

3.1 Rate as a function of the inlet C_2Cl_4 and water vapor concentration

The kinetic of the photocatalytic transformation of C_2Cl_4 was evaluated *i*) at different concentrations of the inlet flow (C_0) and *ii*) at different concentration of water vapor concentration. In both cases under stationary state the conversion was obtained and from this the transformation rate was computed (eq. 1). It is worth mentioning that the rate calculated from the experimental conversion refers to the concentration inside the reactor, and to $C_{out}=C_o(1-\eta)$.

Fig. 1A shows the photonic efficiency (PE) at different C_0, and plotted vs the actual concentration inside the reactor (C_{out}). The photocatalytic efficiency PE is given by the photocatalytic rate [mol m^{-2} s^{-1}] divided by the incoming light irradiance I_o [mol of photons m^{-2} s^{-1}]. The inset in Fig. 1A shows the stationary state (SS) conversion as a function of the inlet concentration of perchloroethylene. As the conversion is almost independent of the inlet concentration, a quasi-first order kinetic was observed ($rate=m\times C_{out}^n$ where n=1 for first order, observed n=0.90).

A basic kinetic approach to the photocatalytic process previously reported [28] and widely discussed,[23] based on 5 primary steps (light absorption with production of an exciton in the bulk, charge carriers migration to the surface, recombination of the charge carriers at the

surface, interface charge transfer of holes to a reduced substrate and conduction band electrons transfer to an oxidant species), gives the *rate*=$\varphi \times QY$, where the quantum yield (QY) of the photocatalytic process is:

$$QY = \left(-y + \sqrt{y\,(y+2)}\right) \qquad \text{(eq. 2)}$$

The master variable y in eq. 2 is formally the ratio of two rates, the chemical rate at the catalyst surface and φ, which is the rate of absorption of photons in units consistent with those of the chemical rate (e.g. mol m^{-2} s^{-1}):

$$y = k_0 \frac{\{C_{red}\}\{C_{ox}\}}{\varphi} \qquad \text{(eq. 3)}$$

where k_0 is a combination of microscopic kinetic constants, and $\{C_{red}\}$ and $\{C_{ox}\}$ are the concentrations of the reduced and oxidized species adsorbed at the surface according to a proper adsorption isotherm (e.g. in the most simplified case a Langmuir isotherm). The above model, where the oxidant and reductant are different species, foresees a reaction order $\boldsymbol{0 \le n \le 0.5}$, often experimentally verified [22,28] and recently deeply tested for the oxidation reaction of formic acid in the presence of oxygen.[29]

The first order observed in the case of PCE (see Fig. 1A) can be rationalized in the framework of the basic kinetic model briefly summarized above considering the possibility that C_2Cl_4 reacts *both* with h_s^+ and e_s^-. This double reactivity of the substrate has been hardly ever considered in the gas-phase halocarbon degradation because *i*) the most of the experiments are carried out in the presence of O_2, *ii*) oxygen is believed to be an efficient electron scavenger and *iii*) the main goal of the photocatalytic processes is the full oxidation (abatement) of the substrate. An effective competition between O_2 and PCE for the photoproduced electrons can be operating also in the presence of excess oxygen as few PCE ppm were able to increase toluene degradation in the presence of air (200000 ppm).[7]

The importance of reductive pathways was proved in aqueous slurry in the study of photo-induced hydrolysis of chlorinated methanes under anaerobic conditions [30], in which the interconversion of CCl_4, $CHCl_3$ and CH_2Cl_2 was supposed to proceed by reductive release of chloride ions. An initial reductive dominance of the reductive pathway was observed for CCl_4 even in the presence of oxygen. Reductants such as alcohols (methanol, propan-2-ol, tert-butanol) remarkably enhance CCl_4 degradation as they scavenge holes.[31] Accordingly, it is worth noting that the early literature reported that compounds exhibiting TCE rate promotion were toluene, ethylbenzene, m-xylene,[7] methyl ethyl ketone (MEK), acetaldehyde, butyraldehyde, methyl tert-butyl ether (MTBE), methyl acrylate, 1,4-dioxane,[32] and methanol.[33] All these compounds are degraded mainly by an oxidative pathway. Then e^-_{CB} scavenging by TCE would increase the rate. Rate inhibition by TCE was exhibited for acetone, methylene chloride, chloroform, and 1,1,1-trichloroethane.[32] These compounds are more likely degraded by a first reduction step like TCE, which then acts as a competitor reducing their transformation rate.

On the hypothesis that C_2Cl_4 reacts *both* with h_s^+ and e_s^-, it is possible to predict that the presence of oxygen is not mandatory for an effective transformation of PCE (*vide infra*), because both surface holes and electrons are able to be scavenged by the substrate itself (i.e $\{C_{red}\}=\{C_{ox}\}$). In this case

$$QY = 2\left(-y + \sqrt{y\,(y+2)}\right) \qquad \text{(eq. 4)}$$

where the master variable $y=k_o\{PCE\}^2/\varphi$. Eq. 4 shows that when the substrate can be simultaneously oxidized and reduced the reaction order is $0 \leq n \leq 1$. The first order at low {PCE} (low value of y and then low value of QY or PE, see Fig. 1) is evident when y value is significantly lower than 2. For this case

$$QY \approx 2\{PCE\}\sqrt{\frac{2k_0}{\varphi}} \qquad \text{(eq. 5)}$$

As the absorbed light is proportional to the incident one ($\varphi = \alpha I_0$), and the photocatalytic rate is given by $rate = \varphi QY$, the photonic efficiency PE= $rate/I_o$ is

$$PE = 2\{PCE\}\sqrt{2\alpha k_0 I_0} = k'\{PCE\} \qquad \text{(eq. 6)}$$

where $k' = \sqrt{8\alpha k_0 I_0}$. This equation justifies the first order rate observed for the PCE photocatalytic transformation (Fig. 1A), and supports the role of the reductive pathway, that will be deeply investigated under anoxic conditions (see below).

The transformation rate of PCE was also investigated at increasing relative humidity. Fig. 1B shows that the rate normalized for the incoming light intensity I_0 decreases with increasing water vapor content, as previously reported when the mole fraction of H_2O is 50–60 times higher than that of PCE.[34] The inhibition of the PCE photocatalytic rate with the increment of the water vapor concentration can be rationalized by considering the competitive adsorption of PCE with water (W) for the same adsorption sites *s,* and can be modeled using a competitive Langmuir isotherm

$$\{PCE\} = \frac{K_{ads}^{PCE}\{s\}[PCE]}{1 + K_{ads}^{PCE}[PCE] + K_{ads}^{W}[W]^n} \qquad \text{(eq. 7)}$$

where { } and [] are concentrations at the surface and in the gas phase, respectively, and $\{s\}$ is the concentration of adsorption sites. The above isotherm can be easily derived using the balance of surface sites and the equilibrium constants of reactions s + PCE ⇆ s-PCE and s + nW ⇆ s-W_n, which are K_{ads}^{PCE} and K_{ads}^{W}, respectively.

Combining equations (6) and (7) the experimentally determined PE is related to the concentration of gaseous water in the reactor by

$$\frac{1}{PE} = a + b\,[W]^n \qquad \text{(eq. 8)}$$

where $a = \frac{1 + K_{ads}^{PCE}[PCE]}{k' K_{ads}^{PCE}\{s\}[PCE]}$ and $b = \frac{K_{ads}^{W}}{k' K_{ads}^{PCE}\{s\}[PCE]}$. In the used experimental conditions a and b are constants ([PCE] = 3 ppm, constant surface area, constant light intensity).

By numerical fit of experimental data $n = 2.2 \pm 0.1$ was obtained, suggesting a displacement of 2 molecules of water for molecule of adsorbed PCE. The dashed curve in Fig. 1B is obtained with n=2.2, a=18.3, b=920 and shows the goodness of the model. Also linearization with eq. 8 has R^2=0.992. The model also predicts that PE is not dependent of the humidity at low water content, supplementing literature data [34] and confirming that traces of water are uninfluential for experiments carried out under dry condition. From the ratio *a/b* and under the reasonable hypothesis that $K_{ads}^{PCE}[PCE] >> 1$ one obtains $K_{ads}^{PCE} = (1.6 \pm 0.2) \times 10^2 K_{ads}^{W}$. Because the dependence of the photocatalytic rate from the water content is highly dependent on the catalyst preparation [35], the reported value refers to the catalyst specimen used in this work.

As H_2O is needed to compensate surface unoccupied atomic orbitals,[36] the calculated value indicates that PCE is strongly adsorbed.

The competitive adsorption of H_2O and C_2Cl_4 on the same reactive sites is a strong proof that the photocatalytic transformation of PCE takes place at the TiO_2 surface, where the direct electron transfer occurs.

As a consequence of the detrimental role of water in the PCE photocatalytic transformation, the below reported experiments were carried out in dry gas. Although under this condition, traces of water are unavoidable, but such traces are uninfluential (see above).

3.2 Basic mechanism

The reactivity (transformation kinetics and by-products) was compared in the presence of synthetic air (N_2 80% + O_2 20%) and in anoxic conditions (N_2 100%) with the aim to give insights on the role of oxidative and reductive pathways. A complete anoxia cannot be reached as a consequence of the ubiquitous atmospheric oxygen which unavoidably diffuses into the reactor and tubes, even though a continuous flow through the reactor with N_2 is fed. This hinders to reach a complete anoxia even at very long irradiation time. On the contrary in an ideal batch reactor in which diffusion of O_2 from the atmosphere is absent, initial traces of oxygen would be easily removed during the photocatalytic process and authentic anoxic condition would be reached. In actual anoxic experimental conditions a residual O_2 concentration ≤ 10 ppm was attained.

Fig. 2A shows the residual concentration of PCE going out of the reactor under irradiation. A significant photocatalytic transformation of PCE was observed both in the presence and in the absence of oxygen with a slightly higher conversion in oxygenated atmosphere. Despite of the most common photocatalytic transformations of organic substrates are completely blocked in the absence of electron scavengers (when $\{C_{ox}\}=0$, in eq. 3 $y = 0$, and consequently QY and the rate are null), the rate of PCE degradation is only partially depressed with oxygen shortage. This supports the previous hypothesis that C_2Cl_4 is able to be concurrently oxidized by holes and reduced by the photoelectrons, as depicted in the following reactions:

$$C_2Cl_{4(ads)} + h_s^+ \longrightarrow C^+Cl_2$$

reaction (r2) and that, in oxic conditions, it reacts in later steps of degradation. Then reductive electron transfer, which occurs only at the catalyst surface, is always operating.

From the comparison between the amount of cumulated chloride and the total amount of PCE photocatalytically transformed in the same time, the molar fraction χ of C_2Cl_4 converted in chloride was computed (ratio between the μmol of C_2Cl_4 degraded and the μmol of deposited chloride, both normalized per unit area). The values of χ are reported as inset in Fig. 2B. In the presence of O_2 larger values of χ were observed, which indicate that PCE is oxidized according to reaction (r1) without losing chloride anion, and later reactions with O_2 increment its degradation rate. Then organic chlorine must be released in some other forms as well as chloride.

The transformation of PCE was investigated on TiO_2 films on which different amount of chloride ion was deposited through evaporation of an aerosol of sodium chloride solution. To prevent that the amount of surface chloride changed significantly during the photocatalyzed reaction, the experiments were carried out at low conversion and shortly terminated (after 10 minutes of irradiation). Fig. 3A shows the PE with and without oxygen as a function of the chloride amount added at the surface. In both oxic and anoxic condition the addition of chloride ion had a detrimental effect on the PCE degradation rate for the reasons already discussed (a redox null cycle or physical occupation of sites, preventing PCE adsorption).

The former hypothesis was that organic chlorine could be released as $Cl^{\bullet}$, which also favors chain reactions useful for further degradation, and that also chloride ion can be oxidized to $Cl^{\bullet}$ radical as mentioned in the Introduction. Then, the production of active chlorine gives insights not only on the role of the surface chloride in the photocatalytic process, but also on some other peculiar aspects of the photocatalytic transformation of PCE.

The production of active chlorine (AC, i.e. $HClO/ClO^{-}$, Cl_2, ClO and ClO_2) in the gaseous phase is reported in Fig. 3B as a function of the irradiation time under the four investigated conditions. Only in the presence of oxygen the production of a significant amount of AC was observed (after a delay time of roughly 30 minutes due to the exponential dilution in the CST reactor) while in anoxic conditions the concentration of AC is lower than the limit of detection. Because in the absence of O_2 the only active chlorine species that can be produced is Cl_2, the transformation of PCE does not involve pathways in which the production of Cl_2 is operational. The absence of Cl_2 excludes that $Cl^{\bullet}$ radicals are produced through oxidation by holes of chloride ion self-released or added as NaCl, or through release from intermediates, and agrees with the absence of $Cl^{\bullet}$ evidenced by EPR spectroscopy.[19] The holes at the surface (h_s^+) have a sufficient redox potential for the oxidation of Cl^{-} to $Cl^{\bullet}$.[17] A possible competition of chloride ion for h^+_{VB} is possible as a decrease of the rate was observed (Fig. 3A). However, this radical is evidently not formed because surface mediated recombination processes with e^-_{CB} could be operational. Then, the suggested production of a significant amount of chlorine radical at the irradiated surface [2,4,39] is not in agreement with the absence of AC observed here without oxygen.

Conversely, in the presence of oxygen there is production of AC. Even if the eventually formed chlorine radical reacts with oxygen to give ClO_2, under irradiation it can be immediately transformed into ClO through its photolysis via the reaction ClO_2 ($^2B_2$) → ClO(2Π) + O(^{3}P) [38], and then the detected AC is composed of HClO and/or ClO. However, because Cl_2 is not formed under anoxic conditions as above reported, there is good reason to assume that only oxygenated species such as $HClO/ClO^{-}$, and ClO are produced in the

presence of oxygen. Furthermore, as no significant difference between the production of AC in the presence of oxygen was observed for the pristine and surface chlorinated catalysts (see Fig. 3B), these species must derive from intermediates, and are produced through their dehalogenation, that is organic chlorine is directly released as HClO or ClO. Then, in the presence of oxygen the operational mechanism for PCE transformation would imply the production of oxygenated chlorinated species.

3.3 Main intermediates

The main by-products of the PCE photocatalytic transformation are those previously reported [2,4,39], namely phosgene, trichloroacetyl chloride (TCAC), tetrachloromethane and esachloroethane. The gaseous species were identified through FT-IR spectrophotometry equipped with a cell with long optical path (8 m) and GC-MS. From FT-IR spectra (see Fig. 3-SM) in the 2500-500 cm^{-1} CO_2, $COCl_2$, traces of TCAC and other unknown chlorinated compounds were detected (see SM under 3.). The identification of the main products was carried out by comparing the recorded spectra with the spectra of pure gaseous standard.[40] From GC-MS with cryofocusing the residual C_2Cl_4, the produced CCl_4 and C_2Cl_6 were detected (see Fig. 4-SM).

Fig. 4A shows the concentration of photocatalytic produced carbon tetrachloride in the presence and absence of oxygen. The presence of chlorides has a detrimental effect on the production of CCl_4 both with and without O_2. The effect is larger under anoxic conditions. The production of CCl_4 is strongly inhibited in the presence of oxygen. The concentration of this molecule increased monotonically during the experiments in both cases, but the concentrations reached in anoxic conditions are roughly 1-2 order of magnitude higher than in the presence of oxygen (see Fig. 5-SM). Then the increase of CCl_4 with irradiation time is *NOT* correlated with the concomitant increase of released chloride observed during the photocatalytic degradation of PCE (see Fig. 2B). CCl_4 must be released from intermediates formed upon further chlorination, favored under anoxic conditions, and the chlorination is not due to chlorine radical, as discussed before.

During the same experiments the evolution of hexachloroethane was also monitored. As for CCl_4, the production of C_2Cl_6 is totally impeded by an excess of oxygen and favored by anoxic conditions. Conversely, chloride ions at the surface favor its production (Fig. 4B). Given that $^{\bullet}Cl$ radical is not present and that the primary reducing step decrements by one the number of organic chlorine, there is the sole possibility that the carbocation $C^{+}Cl_2$

carbocation was demonstrated as necessary to justify observed reaction products.[24] The reaction of an anion with a carbocation, actually formed for direct hole transfer to PCE (reaction r1) and with CCl_3

The mechanism of formation of the detected compounds and of higher MW compounds with conjugated double bonds could be sketched as: 1) the addition of C_2Cl_4 to neutral radical formed upon reduction (r2); 2) the arrangement of the radical by chlorine transposition; 3) loss of CCl_4 (as suggested before). Amongst these steps the oxidation of intermediates by holes forms a carbocation that adds one chloride anion, giving molecules with less double bonds and more chlorine (toward chloroalkanes, as depicted in r4 and r5). Alternatively, amongst these steps, the reduction of intermediates by e_s^- and loss of chloride ion forms a neutral molecule or radical that can undergo the previous reactions. The formation of the detected 1,1,2,3,4,4-hexachlorobuta-1,3-diene is here proposed as an example (see also Fig. 6).

$$CCl_2{=}C^{\bullet}Cl_{(ads)} + C_2Cl_4 \rightarrow CCl_2{=}C(Cl)$$

462 **FIGURE CAPTIONS**

463

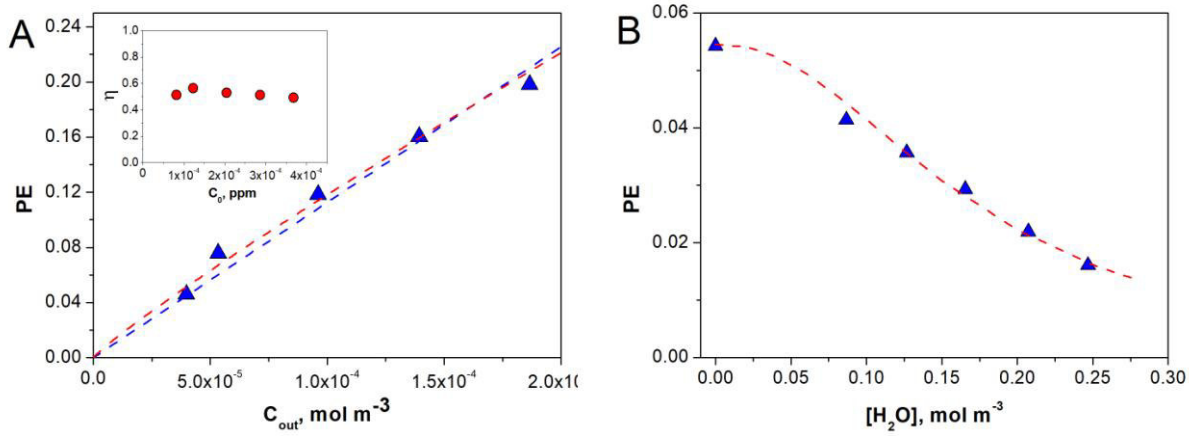

464

465 **Fig. 1**. (A) Photon efficiency PE=rate/I_o of PCE transformation as a function of actual
466 concentration in the reactor. Inset: conversion as a function of inlet concentration C_o.
467 Conditions: C_0 = 2-9 ppm, total flow = 3.0 L min^{-1} (N_2 80%, O_2 20%), S = 15 cm^2, I_o=10 W
468 m^{-2}. (B) Photon efficiency PE of PCE transformation as a function of actual water vapor
469 concentration. The dashed line shows the data interpolation with eq. 8 (see text). Conditions:
470 C_0 = 3 ppm, total flow = 1.6 L min^{-1} (N_2 80%, O_2 20%), S = 15 cm^2, I_o=10 W m^{-2}.

471

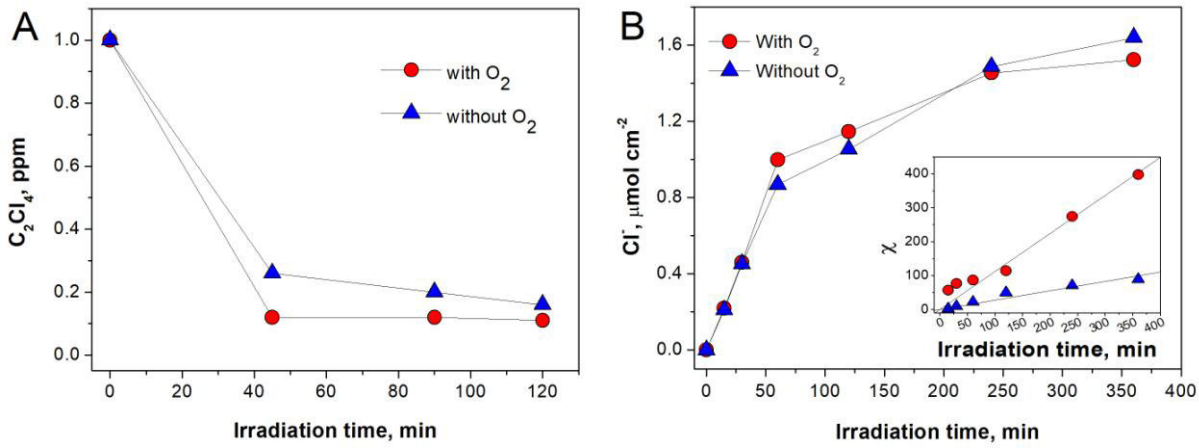

472

473

474

475 **Fig. 2**. (A) residual concentration of PCE going out of the reactor in the presence of
476 oxygen (N_2 80% + O_2 20%) and in quasi-anoxic conditions (N_2 100 %) as a function of the
477 irradiation time. Experimental conditions: C_0 = 1 ppm, total flow = 1.6 L min^{-1} (N_2 80% + O_2
478 20% or N_2 100%), S = 100 cm^2, I_o=10 W m^{-2}, volume sampled in the cryogenic trap = 50 mL.
479 (B) Evolution of the surface concentration of Cl^- as a function of the irradiation time. Inset:
480 molar fraction χ of C_2Cl_4 converted in chloride ion. Experimental conditions: C_0 = 3 ppm,
481 total flow = 1.6 L min^{-1} (N_2 80% + O_2 20% or N_2 100%), S = 15 cm^2, I_o=10 W m^{-2}.

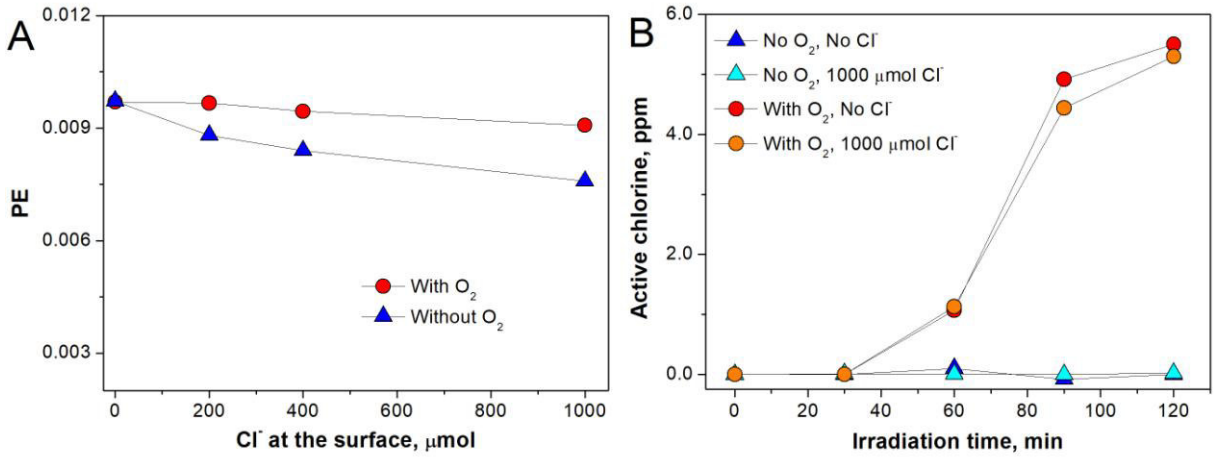

Fig. 3. (A) Photon efficiency PE=Rate/Io for C_2Cl_4 degradation (after 10 minutes of irradiation) in the presence or absence of oxygen as a function of the amount of chloride ions added (as NaCl) at the TiO_2 film surface. Experimental conditions: C_0 = 3 ppm, total flow = 1.6 L min^{-1} (N_2 80% + O_2 20% or N_2 100%), S = 100 cm^2, 10 W m^{-2}. (B) Concentration of active chlorine flowing out of the reactor as a function of the irradiation time in the presence or absence of added chloride (1000 μmol NaCl) at the TiO_2 film surface. Experimental conditions: C_0 = 10 ppm, total flow = 2.4 L min^{-1} (N_2 80% + O_2 20% or N_2 100%), S = 100 cm^2, 10 W m^{-2}.

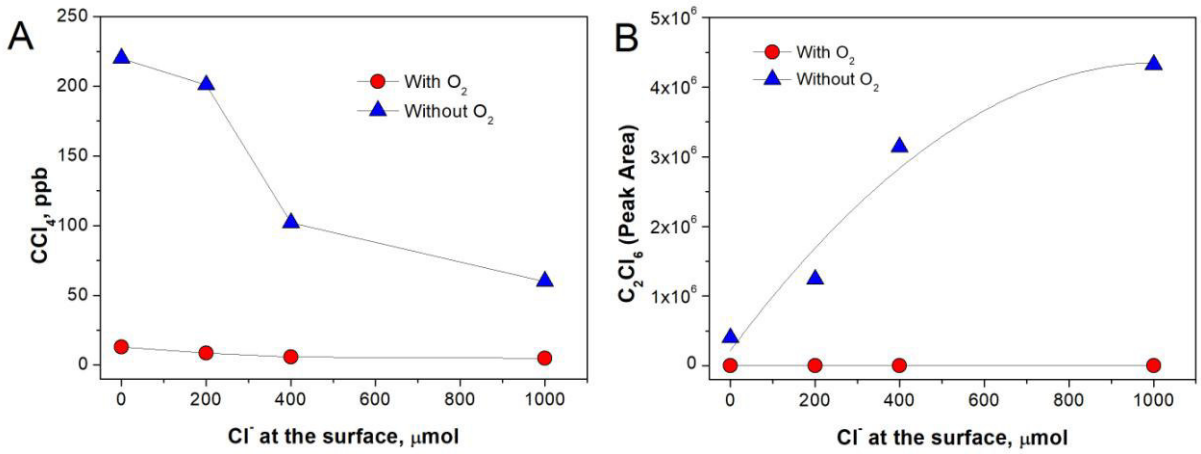

Fig. 4. Concentration of formed CCl_4 (A) and Chromatographic peak area for C_2Cl_6 (B) after 10 minutes of irradiation during the photocatalytic transformation of C_2Cl_4 in the presence or absence of oxygen as a function of the amount of chloride ions added (as NaCl) at the TiO_2 film surface. Experimental conditions: C_0 = 3 ppm, total flow = 1.6 L min^{-1} (N_2 80% + O_2 20% or N_2 100%), S = 100 cm^2, I_o=10 W m^{-2}.

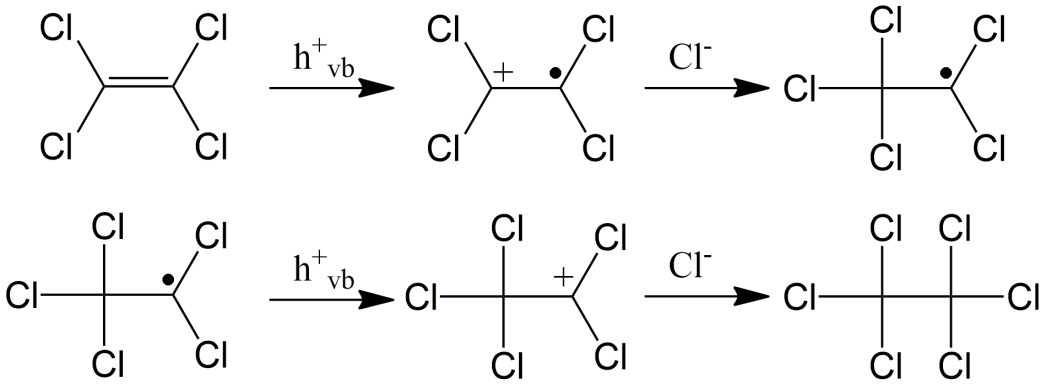

Fig. 5. Mechanism of reaction for the production of C_2Cl_6 during the photocatalytic transformation of gaseous PCE under irradiated TiO_2 in anoxic condition.

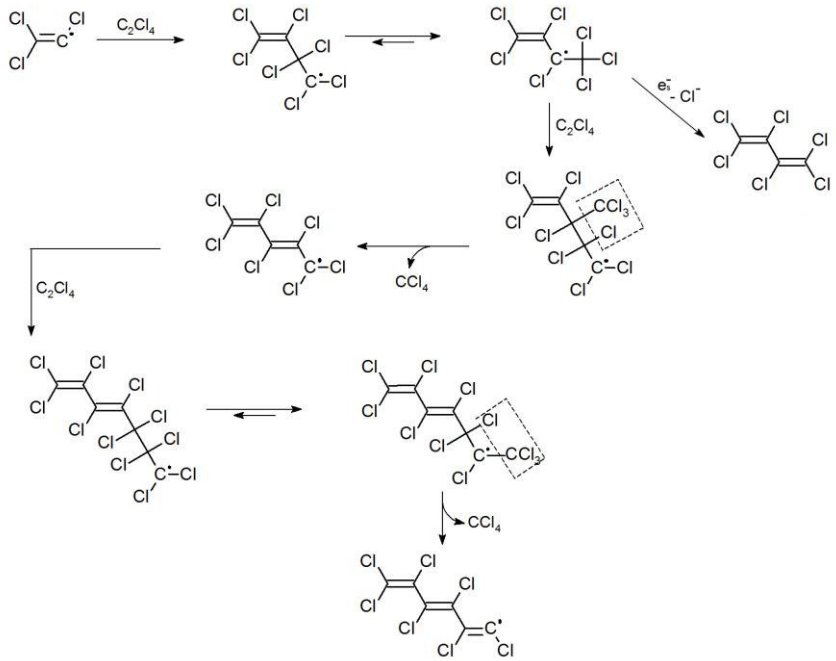

Fig. 6. Suggested mechanism proposed for the production of polyene compounds at the surface of the photocatalyst in anoxic conditions. The structural analogy between the first and the last radicals of the reaction chain allows the perpetuation of the reaction with the production of compounds with higher molecular weight.

512 **References**

[1] W.A. Jacoby, M.R. Nimlos, D.M. Blake, R.D. Noble, C.A. Koval, Environ. Sci. Technol. 28 (1994) 1661-1668.

[2] M.R. Nimlos, W.A. Jacoby, D.M. Blake, T.A. Milne, Environ. Sci. Technol. 27 (1993) 732-740.

[3] S. Yamazaki-Nishida, X. Fu, M. A. Anderson, K. Hori, J. Photochem. Photobiol. A-Chem. 97 (1996) 175-179.

[4] C.-H. Hung, B.J. Mariñas, Environ. Sci. Technol. 31 (1997) 562-568.

[5] J. Peral, D.F. Ollis, J. Catal. 136 (1992) 554-565.

[6] Y. Luo, D.F. Ollis, J. Catal. 163 (1996) 1-11.

[7] M.L. Sauer, M.A. Hale, D.F. Ollis, J. Photochem. Photobiobiol. A: Chem. 88 (1995) 169-178.

[8] S. Yamazaki-Nishida, S. Cervera-March, K.J. Nagano, M.A. Anderson, K. Hori, J. Phys. Chem. 99 (1995) 15814-15821.

[9] R.A.R. Monteiro, A.M.T. Silva, J.R.M. Ângelo, G.V. Silva, A.M. Mendes, R.A.R. Boaventura, V.J.P. Vilar, J. Photochem. Photobiol. A-Chem. 311 (2015) 41-52.

[10] E. Sanhueza, J. Hisatsune, J. Heicklen, Chem. Rev. 76 (1976) 801-826.

[11] M. Anpo, T. Shima, Y. Kubokawa, Chem. Lett. 168 (1985) 1799-1802.

[12] N. Petit, A. Bouzaza, D. Wolbert, P. Petit, J. Dussaud, Catal. Today 124 (2007) 266-272.

[13] O. d'Hennezel, D.F. Ollis, Helv. Chim. Acta 84 (2001) 3511-3518.

[14] P. Wardman, J. Phys. Chem. Ref. Data 18 (1989) 1637-1755.

[15] G. Huybrechts, L. Meyers, Trans. Faraday Soc. 62 (1966) 2191-2199.

[16] L.A. Dibble, G.B. Raupp, Environ. Sci. Technol. 26 (1992) 492-495.

[17] P. Calza, E. Pelizzetti, Pure Appl. Chem. 73 (2001) 1839-1848.

[18] S. Yamazaki, A. Yoshida, H. Abe, J. Photochem. Photobiol. A-Chem. 169 (2005) 191-196.

[19] M. Krivec, R. Dillert, D. W. Bahnemann, A. Mehle, J. Strancara, G. Drazic, Phys.Chem.Chem.Phys. 16 (2014) 14867-14873.

[20] C. Minero, "Surface modified Photocatalysts", in Environmental Photochemistry part III, The Handbook of Environmental Chemistry vol.35, D.W. Bahnemann and K.J. Robertson Eds, 23-44, Springer 2015 – ISBN 978-3-662-46794-7.

[21] J. Fan, J.T. Yates, J. Am. Chem. Soc. 118 (1996) 4686-4692.

[22] V. Maurino, M. Minella, F. Sordello, C. Minero, Appl. Catal. A-Gen. 521(2016) 57-67.

[23] C. Minero, V. Maurino, D. Vione "Photocatalytic mechanisms and reaction pathways drawn from kinetic and probe molecules", in Photocatalysis and Water Purification: from Fundamentals to Recent Applications, 1th ed. – P. Pichat ed., 53-72, Wiley 2013.

[24] M. Bettoni, T. Del Giacco, C. Rol, G.V. Sebastiani, J. Phys. Org. Chem. 419 (2006) 359-364.

[25] C. Minero, A. Bedini, M. Minella, Int. J. Chem. React. Eng. 11 (2013) 717-732.

[26] CEN/TS 16980-1, Photocatalysis - Continuous flow test methods - Part 1: Determination of the degradation of nitric oxide (NO) in the air by photocatalytic materials, (2016)

[27] Standard Methods for the Examination of Water and Wastewater; 20th ed.,American Public Health Association, American Water Works Association, and Water Environment Federation, 1998, Method 4500-Cl G., 4-63; ISO 7393-2:1985, revised 2012 - Water quality -- Determination of free chlorine and total chlorine -- Part 2: Colorimetric method using N,N-diethyl-1,4-phenylenediamine, for routine control purposes.

[28] C. Minero, D. Vione, Appl. Catal. B-Environ. 67 (2006) 257-269.

[29] G. Camera-Roda, V. Augugliaro, A.G. Cardillo, V. Loddo, L. Palmisano, F. Parrino, F. Santarelli, Catal. Today 259 (2015) 87-96.

[30] P. Calza, C. Minero, E. Pelizzetti, Environ. Sci. Technol. 31 (1997) 2198-2203.

[31] P. Calza, C. Minero, E. Pelizzetti, J. Chem. Soc., Faraday Trans. 93 (1997) 3765-3771.

[32] O. d'Hennezel, D.F. Ollis, J. Catalysis 167 (1997) 118-126.

[33] D.S. Muggli, M.J. Odland, L.R. Schmidt, J. Catalysis 203 (2001) 51-63.

[34] S. Yamazaki, H. Tsukamoto, K. Araki, T. Tanimura, I. Tejedor-Tejedor, M.A. Anderson, Appl. Catal. B-Environ. 33 (2001) 109-117.

[35] S. Suáreza, N. Arconada, Y. Castro, J.M. Coronado, R. Portela, A. Durán, B. Sánchez, Appl. Catal. B-Environ. 108-109 (2011) 14-21.

[36] Ulrike Diebold, J. Chem. Phys. 147 (2017) 040901.

[37] S. Yamazaki, T. Tanimura, A. Yoshida, K. Hori, J. Phys. Chem. A 108 (2004) 5183-5188.

[38] J. Thøgersen, P.U. Jepsen, C.L. Thomsen, J.A. Poulsen, J.R. Byberg, S.R. Keiding, J. Phys. Chem. A 101 (1997) 3317-3323.

[39] M. Hegedüs, A. Dombi, Appl. Catal. A-Gen. 271 (2004) 177-184.

[40] NIST Chemistry WebBook, NIST Standard Reference Database Number 69, https://www.nist.gov (last access 14 July 2017).

[41] H. Al-Ekabi, N. Serpone, E. Pelizzetti, C. Minero, M.A. Fox, R.B. Draper, Langmuir 5 (1989) 250-255.

[42] C. Lai, Y.I. Kim, C.M. Wang, T.E. Mallouk, J. Org. Chem. 58 (1993) 1393-1399.

[43] M.B. Smith, J. March, March's Advanced Organic Chemistry: Reactions, Mechanisms, and Structure, Sixth Edition, 2007, John Wiley & Sons, Hoboken, New Jersey.

A revised photocatalytic transformation mechanism for chlorinated VOCs: experimental evidence from C_2Cl_4 in the gas phase

M. Minella, M. Baudino, C. Minero*

Department of Chemistry and NIS Center of Excellence, University of Torino, Via P. Giuria 5, Torino 10125, Italy http://www.environmentalchemistry.unito.it.

* Corresponding author. Tel. +39 0116708449, Fax +39-011-6705242; E-mail: claudio.minero@unito.it.

SUPPLEMENTARY MATERIAL

1 Materials and Methods

1.1 Materials

Titanium dioxide (Hombikat N100: 100% anatase, BET specific surface area 100 m^2 g^{-1}, average crystal size 20 nm) was purchased from Sachtleben Chemie GmbH (Duisburg, Germany). Perchloroethylene (PCE, 99.9%), Titanium(IV) isopropoxide (97%), N,N-Diethyl-p-phenylenediamine (97%), NaOH (≥98%), Na_2HPO_4 (≥98%) and NaH_2PO_4 (99%) were purchased from Sigma Aldrich and absolute ethanol from Fluka (≥98%). Nitrogen was obtained from the evaporation of pure liquid nitrogen (99.999%, SIAD, Italy) while gaseous oxygen (research grade 99.9%) and chromatographic grade Helium (5.5 grade) were supplied by SIAD (Italy). Gaseous standards of PCE were prepared in 15 L SilcoCanTM (Restek) canisters diluting PCE in nitrogen at the desired concentration. All the compounds were used as received without any further purification step. Water was purified with a MilliQ plus apparatus (TOC = 2 ppb, conductivity 18.2 MΩ cm).

1.2 Preparation of the TiO_2 films

TiO_2 films were prepared as follow. 12.5 g of TiO_2 Hombikat N100 were suspended in 50 mL of a Titanium(IV) isopropoxide (TIP, 0.33 mol L^{-1}) in absolute ethanol. 2 mL of the suspension were deposited on the surface of 10×10 cm^2 Pyrex glass substrates, in this way 0.55 g of TiO_2 were deposited on each Pyrex glass substrate as sum of the nanocrystalline catalyst (0.50 g) and the amorphous TiO_2 phase obtained from the hydrolysis of TIP (0.05 g). The samples were dyed at 100 °C for 150 min and UV irradiated (18 W m^{-2} in the 300-400 nm range) for 18 hours with the aim to photocatalytically remove the organic residues from the catalyst surface. The hydrolysis of TIP is essential to obtain a compact and well anchored films. The TiO_2 film samples were storage in the dark and in a closed box to avoid possible poisoning of the surface before use.

1.3 Methods and experimental set-up

The monitoring of C_2Cl_4 flowing out the reactor was carried out with a Photo Ionization Detector PID-AH (from α-Sense with Kr as filling gas for the glow discharge lamp) which signal was amplified (model AD327 amplifier, Analog device), digitalized and recorded by using an analog-to-digital converter (model NI USB-6221, National Instruments).
The volatile VOCs flowing out the reactor were analysed by both GC-MS after cryofocusing and directly by FTIR spectrophotometry.
The cryofocusing system was a Model 7000 Entech system able to focus at the temperature of liquid nitrogen the VOCs, eliminate both CO_2 and water vapour, and inject into the chromatographic system the preconcentrated samples. The GC-MS system used for the VOCs determination was a 6890 GC hyphenated with a 5973 Mass Selective Detector (Agilent Technologies). The column was an Agilent CP-Sil 5 CB column (length 60 m, i.d. 0.32 mm, film thickness 0.1 μm). The analyses were carried out starting from 35°C, increasing the temperature at 5 °C/min up to 140°C and from 140°C to 240°C at 15 °C/min.

Volatile by-products of the PCE photocatalytic transformation were also detected through FT-IR (Cary 670 spectrophotometer, Agilent Technologies) equipped with a cell for gases with 8 m long optical path length. Both the cell and the transfer line were thermostated at 150 °C. The FT-IR spectrophotometer was equipped with a KBr bean splitter and a MCT detector.

The organic compounds cumulated at the catalyst surface in the anoxic conditions were determined through extraction with dichloromethane after irradiation of the film of TiO_2 and

analysed through an Agilent 6890 GC equipped with a GERSTEL CIS4 PTV injector (injection volume 2 μL in splitless mode). The column used was an Agilent HP-5MS (length 30 m, i.d. 0.25 mm, film thickness 0.25 μm). The starting oven temperature was 40 °C for 3 min with a ramp of 5°C/min up to 320 °C (maintained for 9 minutes). The mass spectra obtained were interpreted for comparison with the standard spectra reported in the Wiley 7n library (Agilent part No. G1035B). For both the GC analysis the carrier gas was He of chromatographic grade (Sapio, Italy).

The deposition of water soluble anions at the TiO_2 film surface during the photocatalytic transformation of PCE with and without oxygen was evaluated. After different irradiation times in condition of constant flow of PCE, the films were removed from their Pyrex glass supports, extracted with ultrapure water and the aqueous samples analyzed. The determination of water extractable anions cumulated at the catalyst surface was done through ion chromatography (Dionex 500, with GP40 pump, Rheodyne 9126, 50 μL loop, LC30 oven, ASRS-II Ultra conductivity suppressor and ED40 detector) with the analytical column AS9-HC and column guard AG9-HC. The eluent was K_2CO_3 9 mM, and the flow rate adopted was 1 mL/min keeping the column temperature oven at 30 °C.

Some TiO_2 samples obtained at different irradiation times and conditions were analysed by FT-IR Spectrophotometry to investigate the changes in the surface properties. The samples were pressed in self-supporting pellets ("optical thickness" of ≈ 10 mg cm^{-2}) and placed in an IR cell with KBr windows (Aabspec), permanently attached to a vacuum line (residual pressure = 1.0×10^{-6} Torr), allowing desorption and thermal treatments to be carried out *in situ*. We used a Perkin-Elmer System 2000 FT-IR spectrophotometer equipped with a MCT cryodetector able to record spectra in the 7200-580 cm^{-1} range.

Finally, the UV-Vis reflectance spectra of the film obtained at different irradiation time in the presence of C_2Cl_4 both in oxygen rich and in anoxic conditions were recorded by a Cary 5000 (Varian) spectrophotometer with an integration sphere in polytetrafluoroethyelene (PTFE) with a 150 mm diameter. The elaboration of the %R spectra was carried out by the Kubelka-Munk equation using a PTFE standard sample as reference blank.

1.4 Photochemical reactor and related kinetic treatment

The experiments of PCE transformation were carried out through the experimental set up schematized in Fig. 1-SM. The homemade flow-through photo-reactor worked in a regime of perfect mixing (Continuous Stirred Tank Reactor, CSTR). An internal fan allows the absence of any concentration gradient inside the reactor. The reaction chamber (340×180×90 mm) was in poly-methyl-methacrylate (PMMA) sealed with epoxy glue to avoid air leakage. The cover of the reactor was a Pyrex glass 5 mm thick with a full optical transparency in the emission wavelength range of the adopted light source. A set of two Philips PL-S 9W/2P BLB lamps was used as irradiation source with an emission spectra in the 350-400 nm range with a maximum of emission at 365 nm. To modify the UV irradiance reaching the sample the relative distance between the light source and the sample was properly modified. The light irradiance was measured through a photometer purchased by the Italian vendor CO.FO.MEGRA. The radiative power [W m^{-2}] was converted in the related photon flux [mol of photons m^{-2} s^{-1}] on the basis of the lamp spectrum. A homogeneous irradiation of the whole catalyst surface was always assured. The reactor was built according to the CEN/TS 16980-1:2016 Technical Specification proposed for the Determination of the degradation of nitric oxide (NO) in the air by photocatalytic material.[1] A set of valves allowed the regulation of

the inlet/outlet gas flow and the by-pass of the reactor chamber. The gas flow flowing out the reactors is properly analysed as reported above. For a detailed description of the testing procedure see ref.[2].

The mass balance for C_2Cl_4 in the reactor as a function of the reaction time (for photochemical transformation the irradiation time (t) is

$$V_R \frac{d}{dt} C_{out}(t) = F[C_0 - C_{out}(t)] - S\, Rate(t) \qquad \text{(eq. 1-SM)}$$

where V_R is the reactor volume, $C_{out}(t)$ is the concentration of C_2Cl_4 going out the reactor at the irradiation time t, F is the total flow, S is the geometric area of the TiO_2 film, C_0 is the concentration of the reactant entering the reactor and $Rate(t)$ is the transformation rate normalized for unit area of C_2Cl_4 in the reactor at the irradiation time t.

In condition of steady state (SS, $t \rightarrow \infty$ and no change in the photoactivy of the catalyst, e.g. no poisoning or photo-activation as a consequence of the irradiation) the concentration of C_2Cl_4 does not change with the time ($V_R \frac{d}{dt} C_{out}(t) = 0$) and consequently

$$F[C_0 - C_{out}(t)] - S\, Rate^{SS}(t) = 0 \qquad \text{(eq. 2-SM)}$$

Defining the conversion at the time t as

$$\eta(t) = \frac{C_0 - C_{out}(t)}{C_0} \qquad \text{(eq. 3-SM)}$$

The transformation rate can be expressed as a function of the conversion and so directly measured from the experimental profiles in steady state conditions (eq. 4-SM) [2].

$$Rate^{SS} = \frac{C_0 \eta_\infty F}{S} \qquad \text{(eq. 4-SM)}$$

The inlet gas flows and their concentrations were set with an Entech-4600A Mass Flow Controller (MFC) mixing pure N_2, O_2, and concentrated C_2Cl_4 in N_2. Relative humidity was set by bubbling dry N_2 in thermostated pure water under a fixed pressure.

A thermohygrometric sensor placed in the reaction chamber allowed the determination of both the relative humidity and the temperature. The absolute humidity was computed on the basis of eq. 5-SM [3]

$$p_{H_2O} = 6.11 \frac{RH\%}{100} 10^{\frac{7.5T}{237.7+T}} \qquad \text{(eq.5-SM)}$$

in which p_{H_2O} is the absolute humidity (atm), $RH\%$ is the relative humidity % and T is the temperature (°C). In order to express the absolute humidity in ppm the value of p_{H_2O} [atm] was multiplied for 10^6 (the atmospheric pressure was considered stable and equal to 1 atm).

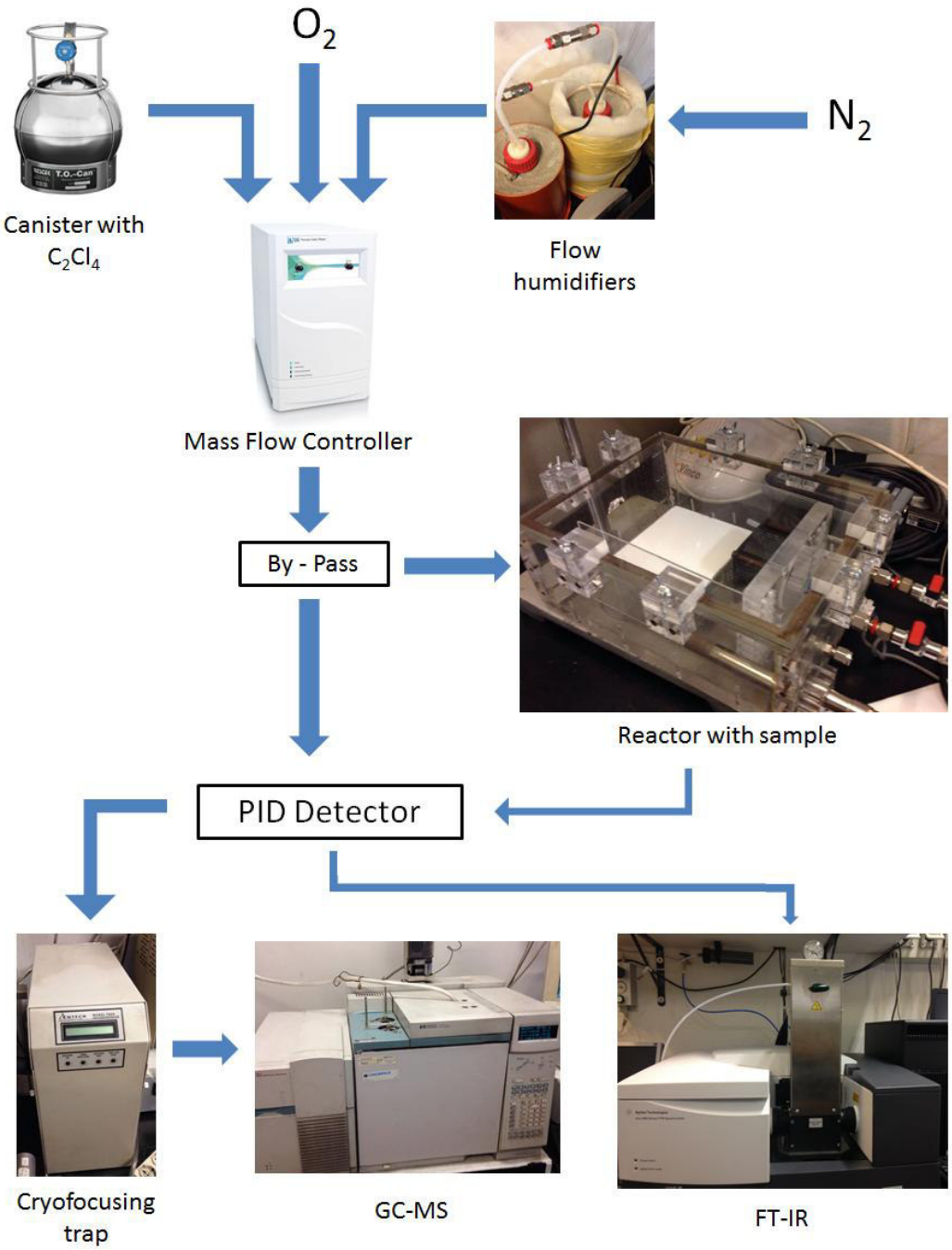

Fig. 1-SM Scheme of the experimental apparatus adopted for the investigation of the photocatalytic transformation of C_2Cl_4.

2 Main Intermediates

Evolution of the amount of oxalate (normalized for the film surface area) deposited on the TiO_2 surface in the presence or absence of oxygen

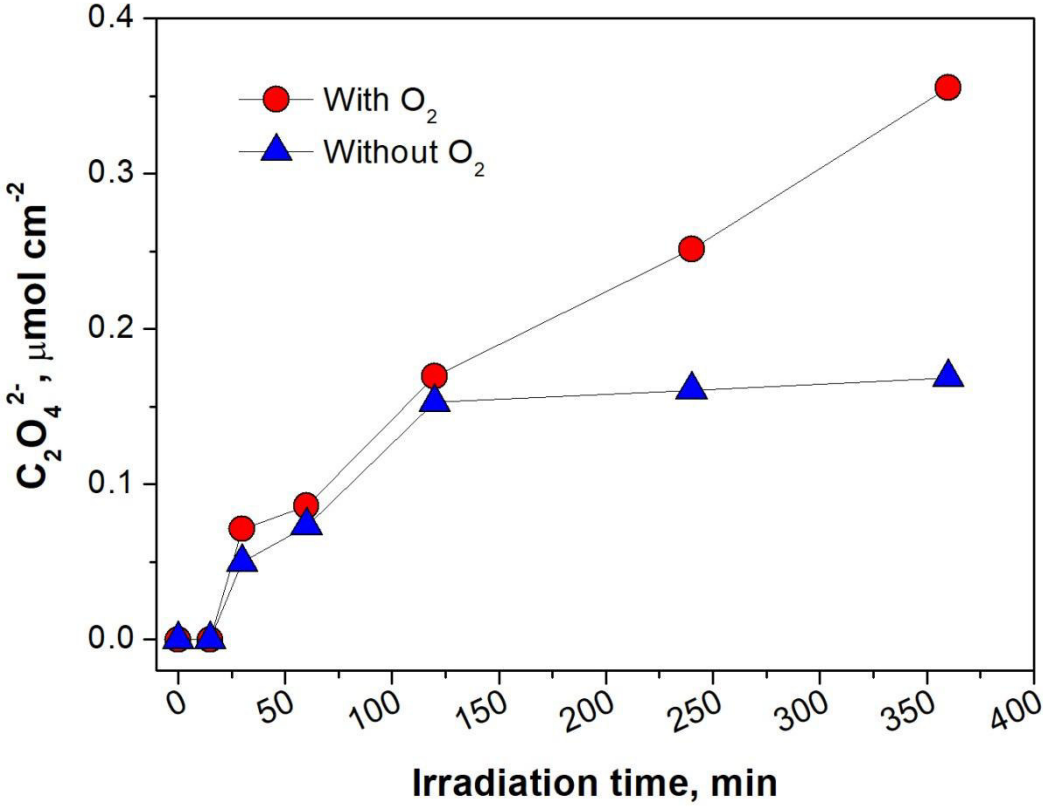

Fig. 2-SM Evolution of the amount of oxalate (normalized for the film surface area) deposited on the TiO_2 surface in the presence or absence of oxygen as a function of the irradiation time during the photocatalytic transformation of gaseous C_2Cl_4. Experimental conditions: C_0 = 3 ppm, total flow = 1.6 L min^{-1} (N_2 80% + O_2 20% or N_2 100%), S = 15 cm^2, 10 W m^{-2}.

3 Detection of gas species

The gaseous species were identified through FT-IR spectrophotometry with long optical path cell (8 m) and GC-MS.
In FT-IR spectra (see Fig. 3-SM) there is the absence of the two main IR signals of the PCE at 914 and 780 cm^{-1} due to the abatement of C_2Cl_4 at concentration lower than the limit of detection of the technique. The main products observed both in the presence and absence of oxygen are carbon dioxide (see the doublet with maxima at 2330 and 2360 cm^{-1} related to its asymmetric stretching) and phosgene (main peaks at 794, 846, 856, 1016, 1680, 1818 and 1834 cm^{-1}). Furthermore, traces of both TCAC and other chlorinated compounds can be hypothesized due to the presence of other minor peaks (e.g. 794, 668 and 569 cm^{-1}) not ascribable to the main transformation products.
The analysis of the by-products formed during the photocatalytic transformation of PCE were carried out also by GC-MS through cryofocusing at the temperature of the liquid nitrogen. The chromatograms obtained (an example is reported in Fig. 4-SM) are dominated by 3 main peaks related to the presence of the residual C_2Cl_4 (t_r = 14.6 min), the photocatalytically produced CCl_4 (t_r = 12.8 min) and C_2Cl_6 (t_r = 28.7 min). The identification of the nature of these compounds were carried out on the basis of the mass spectra (matching between the recorded spectra and the spectra reported in the NIST library ≥ 95%). Note that the absence of phosgene in the chromatogram can be easily explained considering that this compound reacts in the focusing system with the traces of water producing CO_2 and HCl and consequently cannot be determine by the adopted GC-MS system.

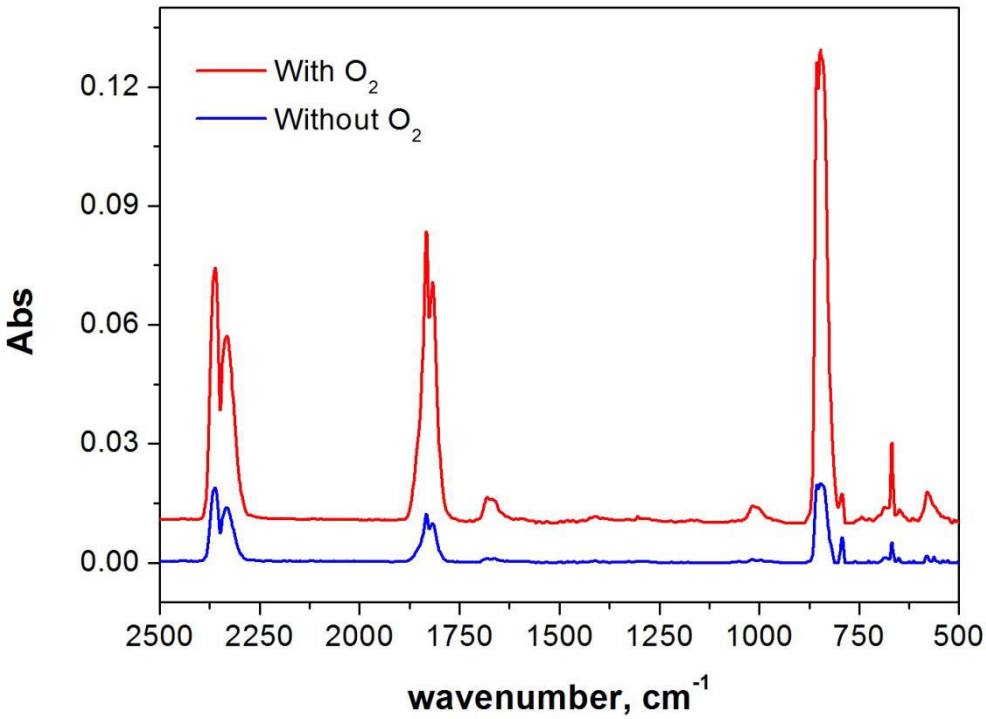

Fig. 3-SM FT-IR spectra in the 2500-500 cm^{-1} range of the gaseous species flowing out of the reactor chamber during the photocatalytic transformation of C_2Cl_4 in the presence of oxygen (red line) and in quasi-anoxic conditions (blue line). Experimental conditions: C_0 = 20 ppm, total flow = 2.0 L min^{-1} (N_2 80% + O_2 20% or N_2 100%), S = 100 cm^2, 10 W m^{-2}, resolution 4 cm^{-1}.

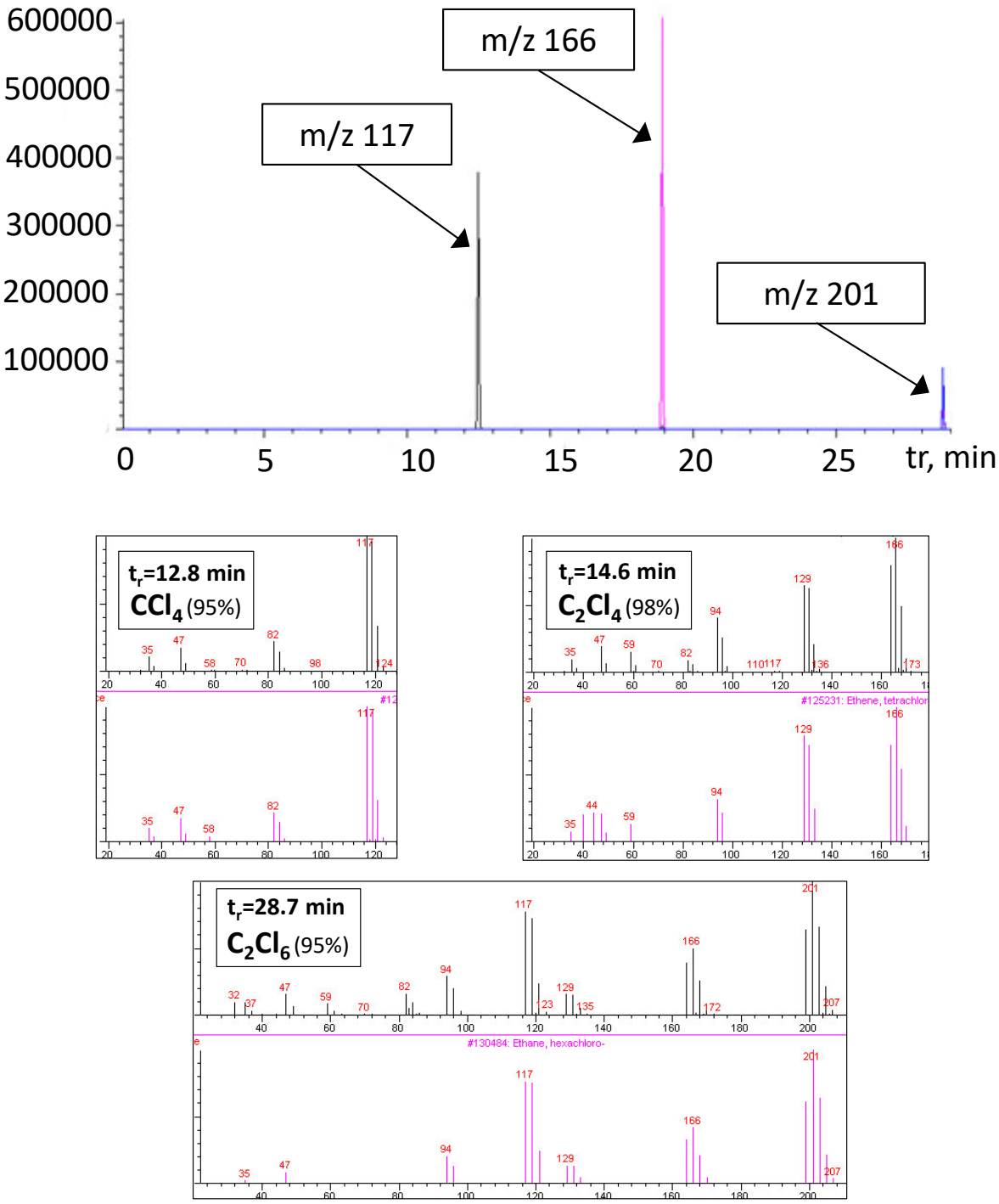

Fig. 4-SM GC analysis of the gaseous species flowing out of the reactor during the C_2Cl_4 photocatalytic transformation under UV-irradiated TiO_2 film. Example of chromatogram (Selective Ion Monitoring (SIM) mode, m/z 117, 166 and 201) and Mass Spectra of the main compounds. For the three compounds identified the related spectra present in the MS library Wiley 7n library were reported together with the goodness of fit (≥95%). Experimental conditions: C_0 = 1 ppm, total flow = 1.6 L min^{-1} (N_2 80% + O_2 20%), S = 100 cm^2, 10 W m^{-2}, volume sampled in the cryogenic trap = 50 mL.

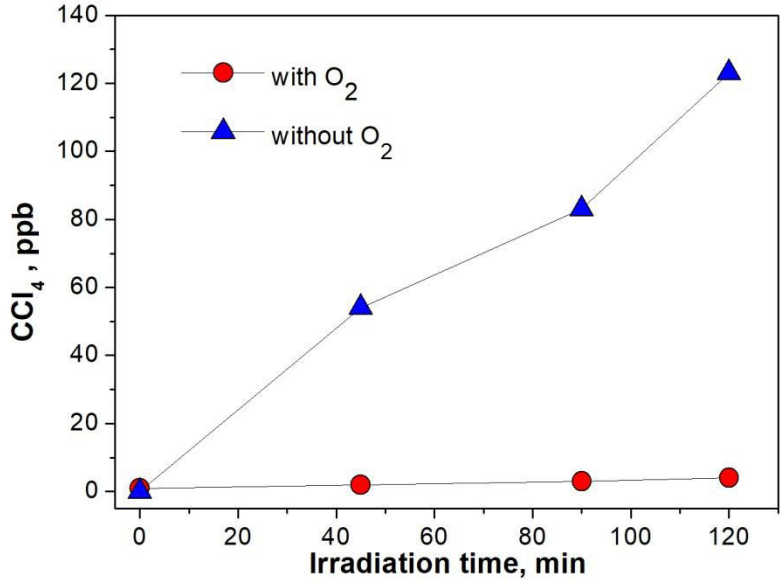

Fig. 5-SM Concentration of the photocatalytically generated CCl_4 (B) in the presence of oxygen (N_2 80% + O_2 20%) and in anoxic conditions (N_2 100 %) as a function of the irradiation time. Experimental conditions: C_0 = 1 ppm, total flow = 1.6 L min^{-1} (N_2 80% + O_2 20% or N_2 100%), S = 100 cm^2, 10 W m^{-2}, volume sampled in the cryogenic trap = 50 mL.

4 Surface species

4.1 UV-Vis reflectance measurements and poisoning

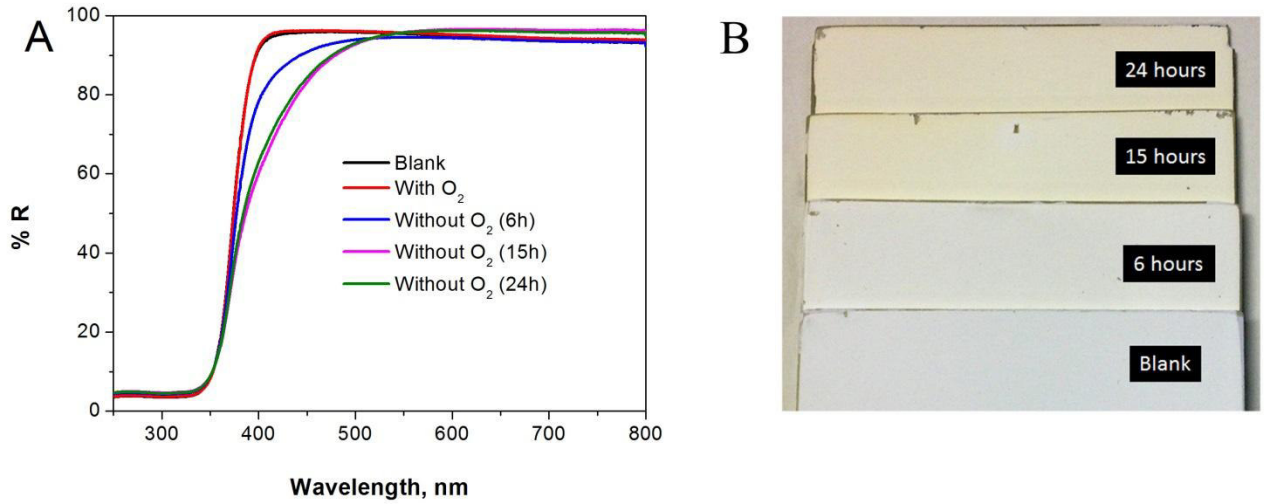

Fig. 6-SM Evolution of the TiO_2 film surface during the photocatalytic transformation of C_2Cl_4 in quasi anoxic-condition under prolonged UV-irradiation (from 0 to 24 hours of continuous irradiation). A) UV-Vis reflectance spectra of the TiO_2 films; B) Pictures of the films obtained after different irradiation times (note the progressive evolution of the surface color toward pale yellow). Experimental conditions: C_0 = 10 ppm, total flow = 2.1 L min^{-1} (N_2 100%), S = 100 cm^2, 10 W m^{-2}.

4.2 Conversion in CSTR in anoxic conditions

During irradiation the experimental conversion in CSTR (after the first transient) decreases, due to poisoning. This effect can't be diagnosed in batch experiments.

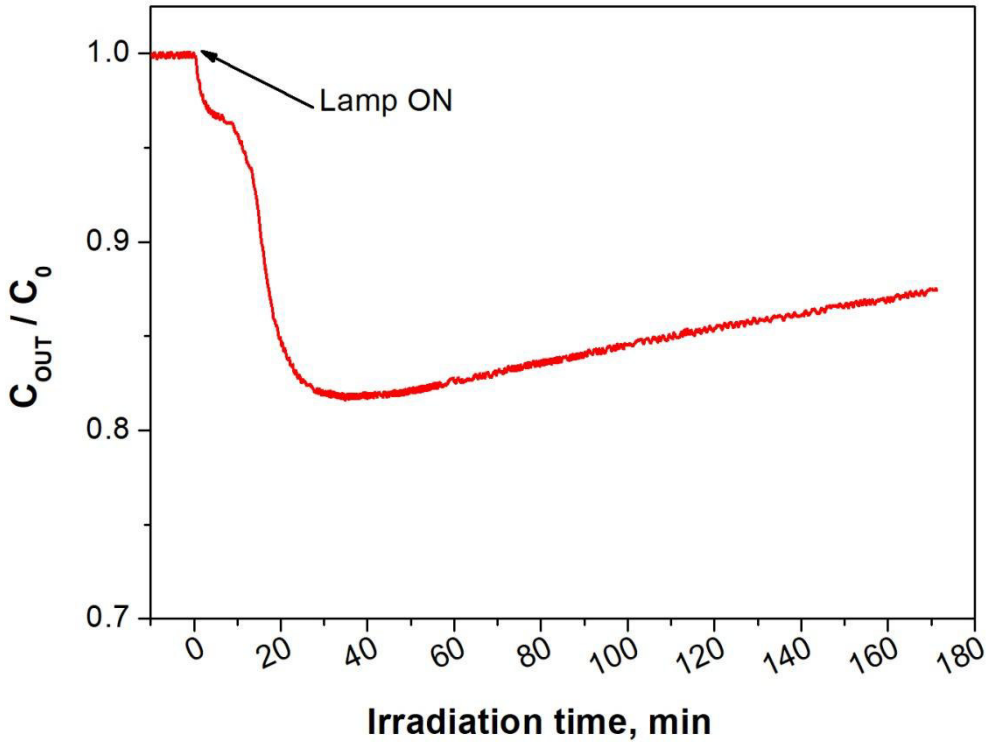

Fig. 7-SM Residual concentration of C_2Cl_4 under anoxic-condition as a function of the irradiation time. Experimental conditions: C_0 = 10 ppm, total flow = 2.1 L min^{-1} (N_2 100%), S = 100 cm^2, 10 W m^{-2}.

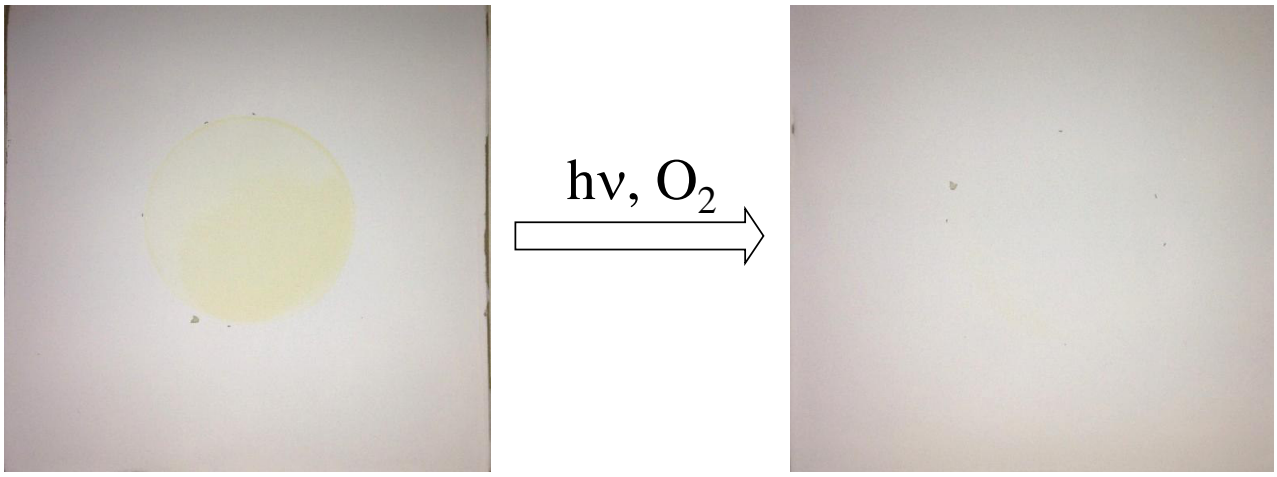

Fig. 8-SM Effect of the irradiation in the presence of oxygen on the TiO_2 film obtained at the end of a long time irradiation in the presence of C_2Cl_4 in quasi anoxic-condition. Note that the yellow-pale compounds deposited during in the anoxic phase disappeared during the irradiation in the presence of oxygen. Experimental conditions: C_0 = 10 ppm, total flow = 2.1 L min^{-1} (N_2 100%), S = 15 cm^2, 10 W m^{-2}.

4.3 FT-IR spectroscopy of surface species

Film samples at different irradiation times were removed from their Pyrex glass substrate and pressed as self-supported pellets. The spectra of the samples in the 1000-4000 cm^{-1} range were recorded after out-gassing at room temperature and at 50 °C for 30 minutes. The spectra of samples before and after 6 hour of irradiation in the presence of oxygen almost overlap (Fig. 9A-SM), indicating a negligible accumulation. The comparison among the spectra obtained after 0, 6, 15 and 24 hours of irradiation in anoxic conditions (Fig. 9B-SM) show a progressive increment of the intensity of: 1) the peak at 1620 cm^{-1} is related to the bending of the water molecules adsorbed at the TiO_2 surface; 2) a new peak formed at 1370 cm^{-1}; 3) the broad absorption band spread over the 3550-2500 cm^{-1} interval and the partly resolved components between 3750 and 3550 cm^{-1}.

As already stated, water traces are always present in the experimental system. The peaks in 3550-2500 cm^{-1} interval are attributed to O–H stretching bond of hydroxyl surface groups (linear or bridged) and adsorbed water. The pattern at 3750-3550 cm^{-1} is commonly attributed to free νOH oscillators while the broad band at 3550-2500 cm^{-1} to H-bonded νOH oscillators.[4,5] The increment of the intensity of these signals, together with the concomitant increment of the 1620 cm^{-1} peak can be related to the increase of the hydration state of the TiO_2 surface. The higher amount of surface water can be related to the presence at the surface of species able to increase the Lewis acidity, and consequently to increase the ability to adsorb water molecules [5], and to the production of water soluble species (e.g. Cl^-), which are able to decrease the vapor tension of the water multilayers located at the TiO_2 surface, and consequently hinder their desorption.

The 1370 cm^{-1} peak can be attributed to the vibration modes of C–Cl bond closed to carbon/carbon double bonds. As an example, 3-chloropropene shows an intense absorption band in the same region with a maximum located at 1417 cm^{-1}.[6] Then compounds of similar structure are cumulated, most probably with increased conjugated double bonds as Vis absorption is developed with irradiation time.

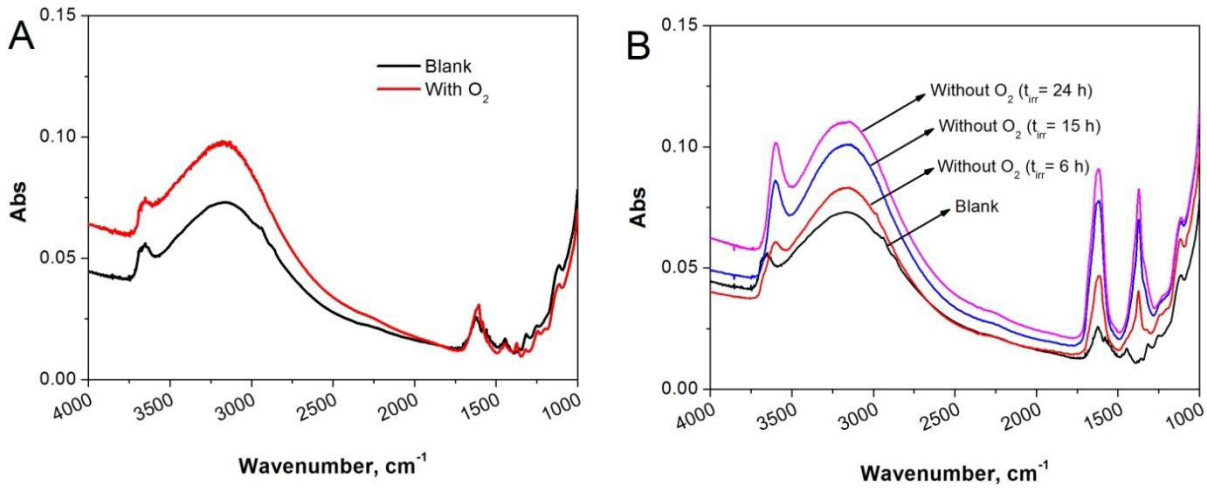

Fig. 9-SM Evolution of the FT-IR spectra of the TiO_2 films removed from the support and analyzed as self-supported pellets during the photocatalytic transformation of C_2Cl_4. (A) Comparison between the samples before and after 6 hour of irradiation in the presence of oxygen; (B) Comparison among the spectra before and after 6, 15 and 24 hours of irradiation in quasi-anoxic conditions. Experimental conditions: C_0 = 10 ppm, total flow = 2.1 L min^{-1} (N_2 80% + O_2 20% or N_2 100%), S = 100 cm^2, 10 W m^{-2}.

4.4 GC-MS analysis of surface species

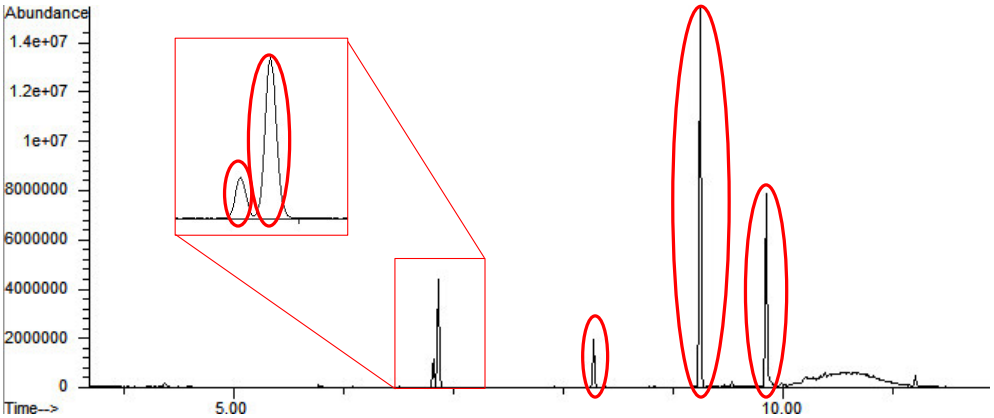

Fig. 10-SM Gas chromatogram (TIC mode) of the sample obtained extracting with CH_2Cl_2 the TiO_2 film after the photocatalytic transformation of C_2Cl_4 in quasi-anoxic condition (C_0 = 10 ppm ppm, flow = 2100 cm^2 (N_2 100%), S = 100 cm^2). The peaks of the five main compounds formed are highlighted in red.

Table 1-SM Retention time, molecular weight and molecular structure of the 5 compounds formed and deposited on the TiO_2 film during the photocatalytic transformation of C_2Cl_4 under irradiated TiO_2 film in quasi-anoxic conditions (C_0 = 1 ppm ppm, flow = 1600 cm^2 (N_2 100%), S = 100 cm^2).

t_r (min)	Compounds		Molecular weight
6,81	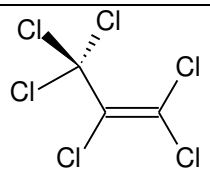		249
	1,1,2,3,3,3- hexachloropropene		
6,85	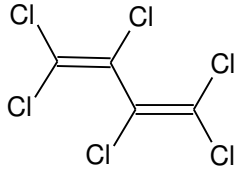		261
	1,1,2,3,4,4-hexachlorobuta-1,3-diene		
8,24	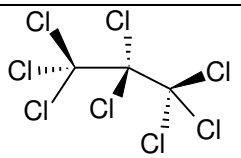		320
	perchloropropane		
9,24 - 9,84	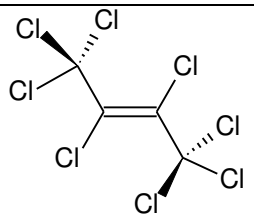	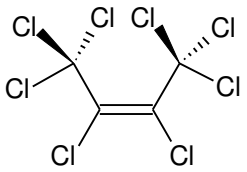	332
	Trans-1,1,1,2,3,4,4,4-ottachlorobut-2-ene	*Cis-1,1,1,2,3,4,4,4-ottachlorobut-2-ene*	

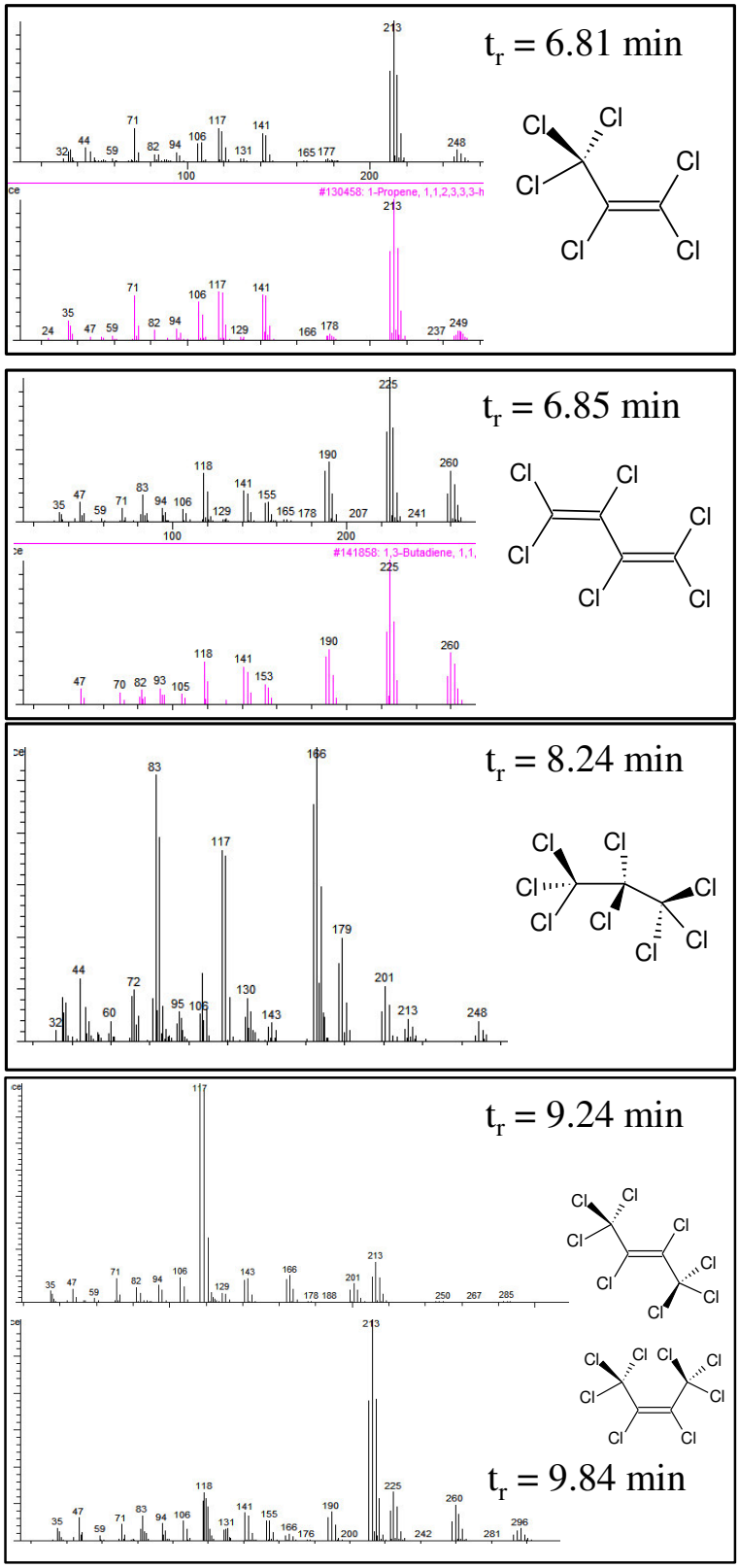

Fig. 11-SM Mass spectra of the molecules formed during the photocatalytic transformation of C_2Cl_4 under irradiated TiO_2 film in quasi-anoxic conditions (C_0 = 1 ppm ppm, flow = 1600 cm^2 (N_2 100%), S = 100 cm^2). For the compounds with t_r = 6.81 and 6.85 min the spectra present in the MS library Wiley 7n library for the related compounds were reported for comparison with the experimental data.

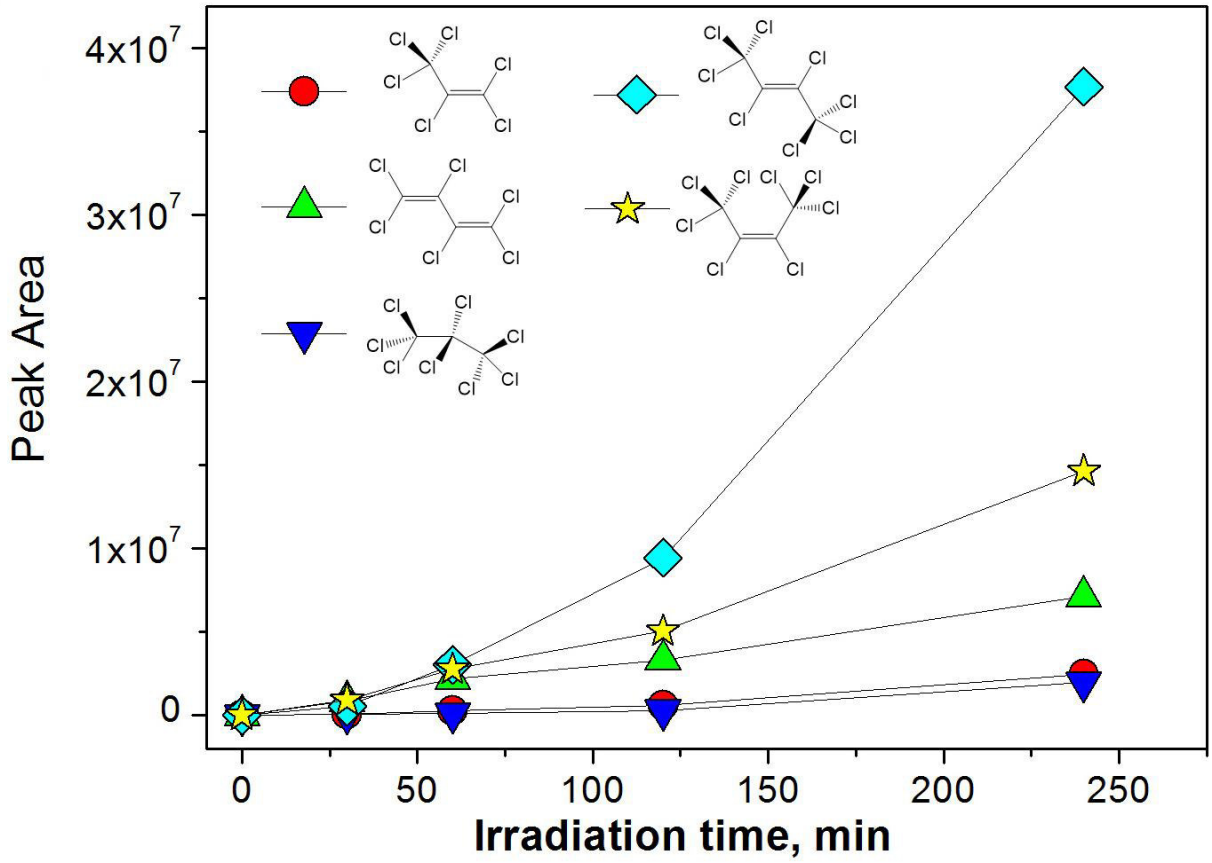

Fig. 12-SM. Area of the peaks of species formed during the photocatalytic transformation of C_2Cl_4 and deposited on the TiO_2 films under anoxic condition as a function of the irradiation time. Experimental conditions: C_0 = 10 ppm, total flow = 2.1 L min^{-1} (N_2 100%), S = 100 cm^2, I_o=10 W m^{-2}.

5 References

[1] CEN/TS 16980-1 Photocatalysis - Continuous flow test methods - Part 1: Determination of the degradation of nitric oxide (NO) in the air by photocatalytic materials, Brussels, Belgium 2016.
[2] C. Minero, A. Bedini, M. Minella, Int. J. Chem. React. Eng. 11 (2013) 717-732.
[3] D. Andrews, An Introduction to Atmospheric Physics, Cambridge University Press, 2010.
[4] M. Primet, P.P. Pichat, M.V. Mathieu, J. Phys. Chem. 75 (1971) 1216-1220.
[5] M. Minella, M. G. Faga, V. Maurino, C. Minero, E. Pelizzetti, S. Coluccia, G. Martra, Langmuir 26 (2010) 2521-2527.
[6] NIST Chemistry WebBook, NIST Standard Reference Database Number 69, https://www.nist.gov (last access 14 July 2017).